Section 2
PROGRESS IN LASER FUSION

2.A Convective-Stimulated Raman-Scattering Instability in UV-Laser Plasmas

It is well known that a number of laser-driven instabilities exist in the corona of laser-produced plasmas.[1] In these instabilities, the incident electro-magnetic (e-m) wave typically decays into a scattered e-m wave of lower frequency and a plasma wave (SRS), or into two-plasma waves ($2\,\omega_p$ decay instability), or into a scattered e-m wave having little or no red shift and an ion-acoustic wave (SBS). All these processes are three-wave processes. Four-wave processes such as self-focusing and modulational instability may also be excited in the corona. The existence of any of these instabilities presents potential problems for laser fusion as they may cause excessive energy loss (SBS), the generation of energetic electrons leading to target preheat (SRS and $2\omega_p$ decay instability), and strong intensity nonuniformities (four-wave processes).

If the existence of some of these instabilities is paired with the necessary theoretical understanding of the processes involved, the experimental signatures of these instabilities may serve as a convenient coronal plasma diagnostic. This is the case with convective SRS which occurs in the underdense corona at $n_e < n_c/4$. In this article, we present some highlights of experiments on SRS backscattering and the theoretical background used to explain the observations. We then apply the theory to obtain time-resolved coronal temperatures from the evolution of the SRS spectra during the laser irradiation interval.

To study SRS backscattering from plane plastic targets, we used the GDL-UV laser facility which delivered up to 50 J in either 0.5 or 1 ns

FWHM pulses at $\lambda = 351$ nm. Intensities on target ranged from 10^{13} to 2×10^{15} W/cm^2. The SRS light backscattered through the lens was extracted from the incident beam path with a dichroic mirror (Fig. 1). This SRS light was then incident on a 1/4 m spectrometer along with a properly timed fiducial derived from the incident beam. The spectrum thus produced was time-resolved with a Hadland 675 ps streak camera with 10 to 20 ps resolution. The work reported here is previously reported work.[2,3]

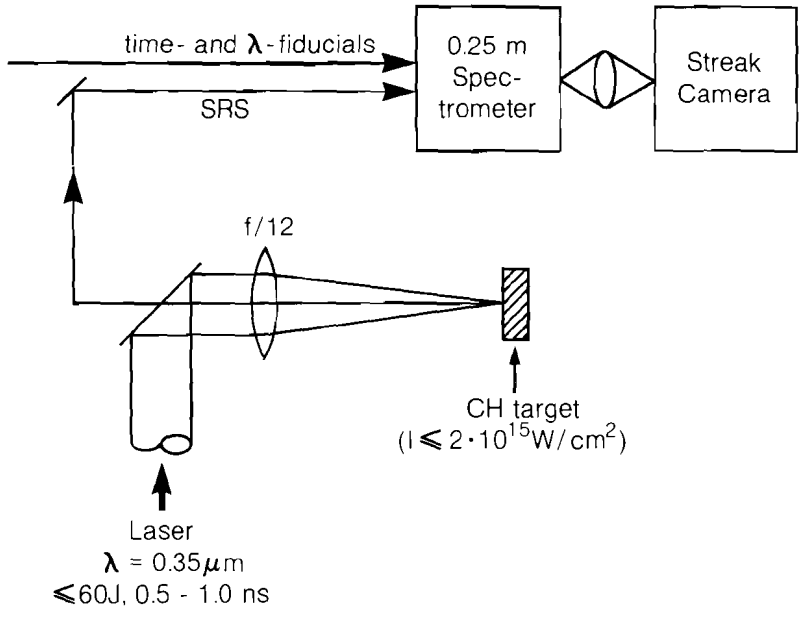

Fig. 1
Experimental set-up for time-resolved SRS backscatter spectra.

A typical time-resolved spectrum is shown in Fig. 2 for a 0.5 ns pulse at 10^{15} W/cm^2 on target. Three distinct components are seen in these spectra: (a) a component due to convective SRS around 450 to 550 nm, (b) $\omega/2$ radiation due to reradiation from the 2 ω_p decay instability at 720 nm, and (c) the delayed incident laser fiducial at 720 nm (second order of fundamental), used for timing and for calibration of wavelength.

In this report, we will concentrate on the interpretation of the SRS signal. This radiation originates in the corona at densities $0.01 < n_e/n_c < 0.2$. Figure 3 schematically depicts the plasma corona with the incident laser penetrating into the dense plasma up to n_c. In the region where convective SRS occurs, the incident e-m wave may decay into a scattered e-m wave and an electron plasma wave, both obeying the energy and momentum conservation laws as well as the relevant dispersion relations (Fig. 3). The corresponding vector diagram is shown in the insert. We note that due to the weak scaling of the frequency of the plasma waves with k_p, we obtain essentially monochromatic, isotropically scattered light at any particular plasma density.

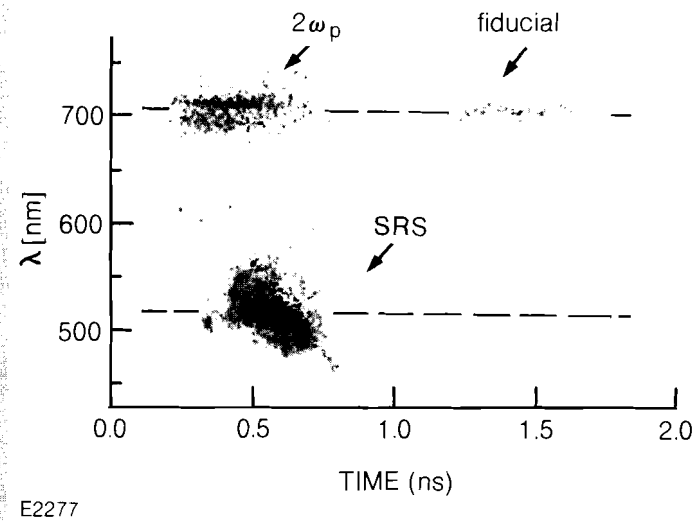

Fig. 2
Typical time-resolved SRS spectrum obtained from plastic (CH) targets at 10^{15} W/cm². The different features are due to convective SRS (450-550 nm), re-radiation from the $2\omega_p$ decay instability (double line at 720 nm), and a timing and wavelength fiducial derived from the incident beam (2 x 351 nm).

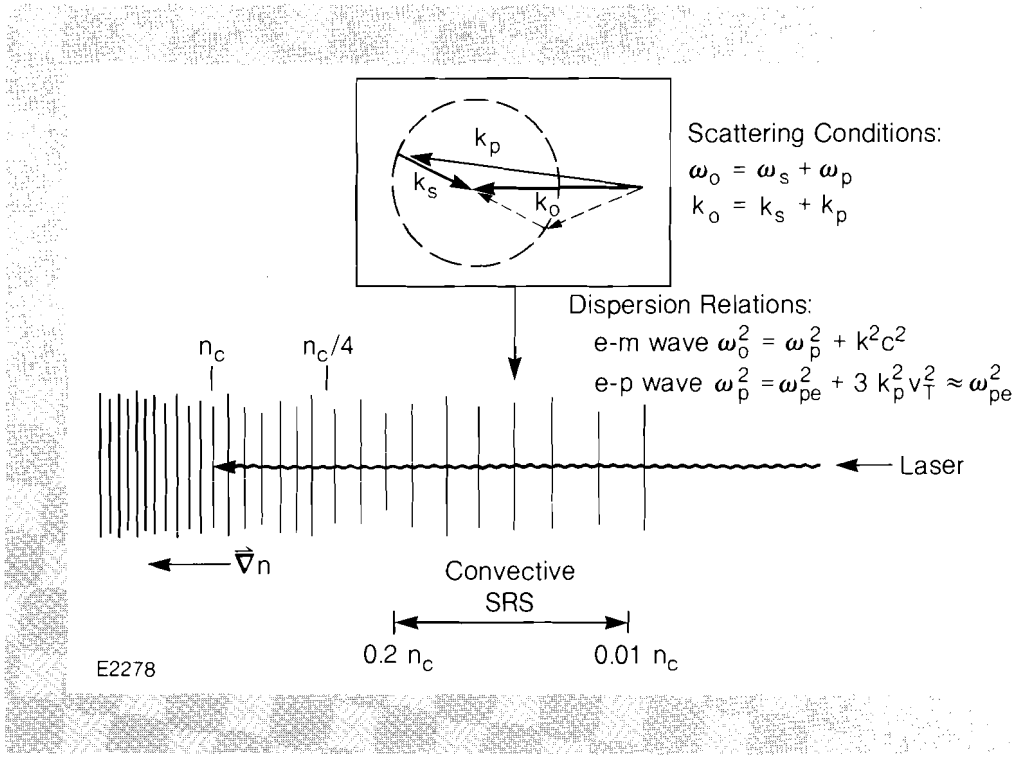

Fig. 3
Schematic diagram of the plasma corona showing typical regions over which SRS is observed. The inset shows a representative k vector diagram for the parametric SRS process. The governing laws for the conservation of energy and momentum and the relevant dispersion relations are also indicated.

However, the scattered light frequency is quite sensitive to the density at which the scattering occurs since $\omega_p \approx \omega_{pe} \propto \sqrt{n_e}$ and $\omega_s = \omega_o - \omega_p \approx \omega_o[(n_e/n_c)^2]$. This results in $\omega_o/2 < \omega_s < \omega_o$. Here the symbols ω_o, ω_s, ω_p, ω_{pe}, are the angular frequencies, respectively, of the incident and scattered e-m waves, the electron plasma wave, and the electron plasma frequency. The electron density is denoted by n_e, and n_c is the critical density at which $\omega_{pe} = \omega_o$. (For typical

coronal temperatures of 1 to 3 keV the thermal correction factor in the dispersion relation for the plasma waves is very small.)

The SRS intensity observed depends on a number of factors: the thermal e-m noise level, the SRS gain coefficient, and the incident light intensity, through

$$I_{SRS} = I_{noise} e^{2\pi G_{SRS} I_L}, \quad (1)$$

where I_{SRS}, I_{noise}, I_L, are, respectively, the SRS, thermal e-m noise, and incident laser intensities. G_{SRS} is the convective SRS gain factor. The threshold intensity for this process, I_{th}, is traditionally[1] defined by $G_{SRS} \cdot I_{th} = 1$. The thermal e-m noise intensity is strongly frequency-dependent and is obtained by correcting the plasma black body spectrum for the optical depth between the density at which the SRS takes place, and the critical density at the frequency of interest. In Fig. 4 we have plotted the wavelength-dependent e-m noise intensity along with typical SRS gain factors. The latter show a short-wavelength cut-off which strongly depends on the coronal electron temperature and is due to electron Landau damping of the plasma wave generated in the SRS process. These gain factors were recently obtained by E. A. Williams[4] by analyzing the existing homogeneous theory of SRS and extending it to inhomogeneous plasmas.

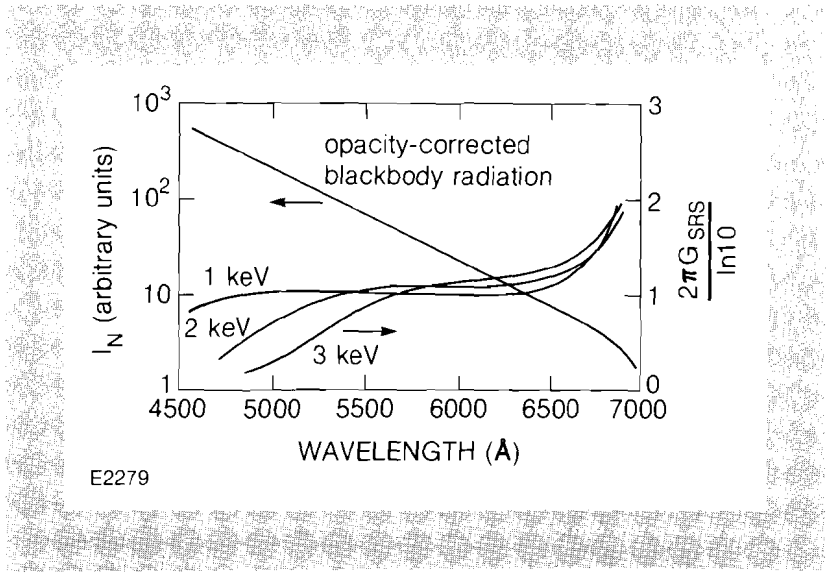

Fig. 4
Wavelength dependence of the e-m noise intensity from which the convective SRS grows, along with calculated[4] SRS gain coefficients. The short-wavelength cut-off is due to electron Landau damping.

Folding the gain factors and the e-m noise intensities according to Eq. (1), one obtains SRS spectra for different temperatures as shown in Fig. 5. These spectra generally exhibit a strongly temperature-dependent short-wavelength cut-off due to the corresponding behavior of the SRS gain coefficient. Close to threshold these spectra also exhibit rather narrow (20-70 nm) distributions whose peaks shift to longer wavelength as the temperature increases. By plotting the wavelengths of the peaks of the calculated spectra as a function of the coronal electron temperature, one obtains the curve shown in Fig. 6. Thus, by estimating the time-dependent wavelengths of the peaks of the experimental spectrum in Fig. 2, one can estimate the coronal temperature evolution during the laser pulse. The range of experimental temperatures thus obtained is

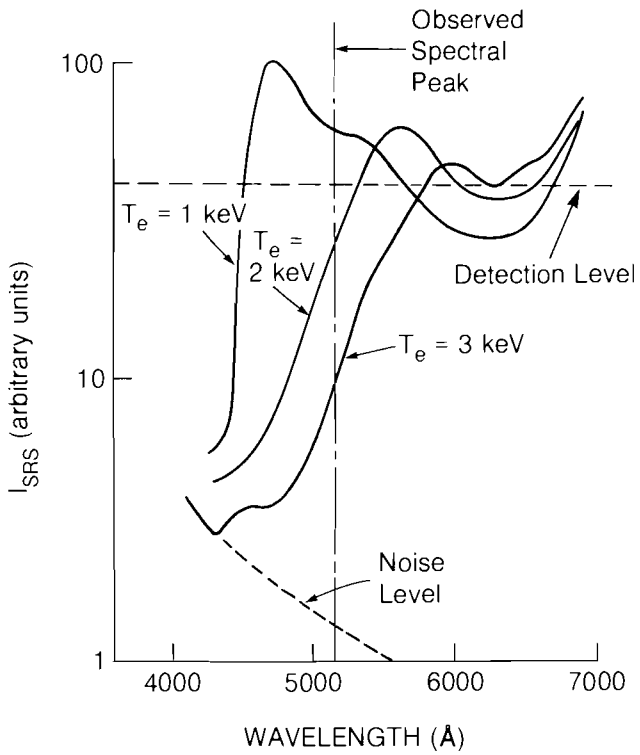

Fig. 5
Calculated SRS spectra near threshold. The strong temperature dependence of the peaks is clearly evident.

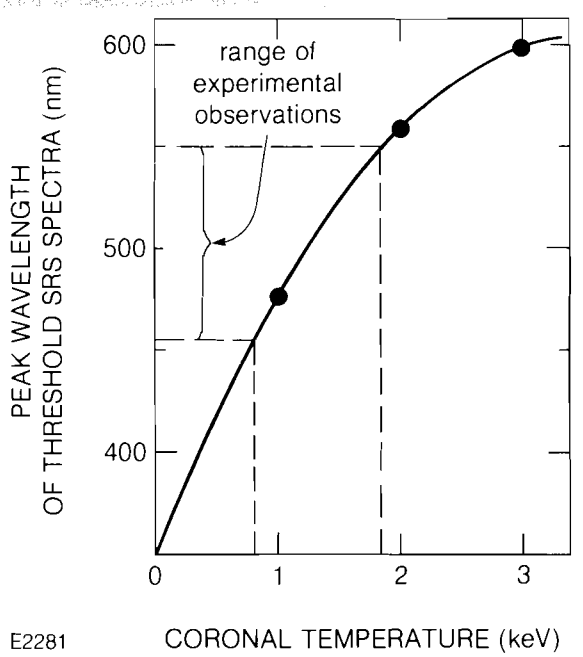

Fig. 6
Temperature dependence of the short-wavelength peaks of the SRS spectra near threshold. Also indicated are the maximum wavelengths observed experimentally for these peaks for 0.5 and 1 ns irradiation. In addition, typical ranges are shown for the coronal temperatures deduced from the experiments.